

Thermodynamic analysis of the solvent effect on tautomerization of acetylacetone: An ab initio approach

Tateki Ishida, Fumio Hirata, and Shigeki Kato

Citation: *J. Chem. Phys.* **110**, 3938 (1999); doi: 10.1063/1.478249

View online: <http://dx.doi.org/10.1063/1.478249>

View Table of Contents: <http://jcp.aip.org/resource/1/JCPSA6/v110/i8>

Published by the AIP Publishing LLC.

Additional information on J. Chem. Phys.

Journal Homepage: <http://jcp.aip.org/>

Journal Information: http://jcp.aip.org/about/about_the_journal

Top downloads: http://jcp.aip.org/features/most_downloaded

Information for Authors: <http://jcp.aip.org/authors>

ADVERTISEMENT

physicstoday

Comment on any
Physics Today article.

The image shows a red arrow pointing from the text 'Comment on any Physics Today article.' to a comment box on a sample article page. The sample article is titled 'Measured energy in Japan' by David von Seggern. The comment box contains the following text:

Comment on this article

By the act of hitting a ball with a bat, one calculates the force energy to deliver the ball to its new location, but one must also take into account that the ball extended its energy release to that which became struck by the ball as its momentum ceased and passed energy to the struck item. Therefore the parameters of the damage extend into the future when the received energy to that pushed upon, later becomes released in a new event. Perhaps calculations of one added that in, while another's calculations did not. E.M.C.

Written by Edgar McCarroll, 14 July 2012 19:59

Thermodynamic analysis of the solvent effect on tautomerization of acetylacetone: An *ab initio* approach

Tateki Ishida

Department of Chemistry, Graduate School of Science, Kyoto University, Kitashirakawa, Sakyo-ku, Kyoto 606, Japan

Fumio Hirata

Institute for Molecular Science, Myodaiji, Okazaki, Aichi 444, Japan

Shigeki Kato

Department of Chemistry, Graduate School of Science, Kyoto University, Kitashirakawa, Sakyo-ku, Kyoto 606, Japan

(Received 16 September 1998; accepted 17 November 1998)

The keto-enol tautomerism of acetylacetone in solution is studied with the reference interaction site model self-consistent-field (RISM-SCF) method. We choose three solvents, H₂O, dimethyl sulfoxide (DMSO), and carbon tetrachloride (CCl₄), representing, respectively, protic polar, aprotic polar and nonpolar solvents. The analysis is made taking account of the solute electronic as well as geometrical change of the tautomers due to solvent effect. In addition, the electronic correlation energy of solute molecule and solute vibrational energies are considered. The free energy differences are analyzed by decomposing them into the enthalpy and entropy terms. The theory reproduces the total free energy determined by the experiment fairly well. We also find that, as solvent polarities increase, the keto tautomer shows the drastic geometric change in order to make its dipole moment larger and that the geometric change of the keto tautomer is enthalpically driven in H₂O and entropically in DMSO. It is made clear that these depend on the solvent property—protic or aprotic. © 1999 American Institute of Physics. [S0021-9606(99)50708-3]

I. INTRODUCTION

Chemical equilibria and reactions in solution have been two of the most important subjects in theoretical chemistry, and various methods have been developed for studying such problems.¹ Computer simulation studies employing molecular dynamics and Monte Carlo techniques have provided a wealth of information on the thermodynamic properties for various processes in solution. Analyses of the solvation free energies derived from these simulations have been utilized for interpreting the origin of thermodynamic stability of chemically equilibrated systems at a molecular level.¹ It has also been emphasized that the electronic structure of solute molecule and the geometry itself are largely influenced through the interaction with surrounding solvent molecules.² In this respect, quantum chemical methods incorporating the solvation effects in the electronic structure calculations of solute have also been advanced to elucidate the importance of the solute electronic polarization effect for understanding the mechanism of chemical equilibria in solution.^{2,3}

The keto-enol tautomerization is among the most well-studied subjects both from experimental and theoretical points of view. Theoretical calculations have so far been performed for some specific systems such as formamide^{4,5} and 2-pyridone,⁵ and many of them have been based on the dielectric continuum model characterizing the solvent by the dielectric constant. In the present work, we performed a theoretical study on the keto-enol tautomerization of acetylacetone in polar and nonpolar solvents using the reference interaction site model self-consistent-field (RISM-SCF)

method,^{6,7} which is an *ab initio* electronic structure theory taking account of the solvent reaction field in molecular detail.

The keto-enol tautomerization of acetylacetone, a prototype β -diketone, has been extensively studied experimentally,^{8–13} and the attention has been paid to its solvent effect. Although the enol form is more stable than the keto in the gas phase due to the intramolecular hydrogen bonding, the equilibrium is known to shift toward the keto in solution as the solvent polarity increases.^{14–18} Several theoretical studies of acetylacetone have been carried out. Dannenberg and Rios¹⁹ employed various levels of *ab initio* electronic structure methods to predict the geometries and stabilities of the keto and enol tautomers in the gas phase. Solvent effects on the tautomerism have also been studied with the self-consistent reaction field method (SCRF),^{20–22} in which a semiempirical level of electronic structure calculations was used. Most importantly, Cramer and Truhlar predicted²³ that the keto form could cause a large geometric change so as to increase the solute dipole moment in polar solvents. However, as mentioned by them, more elaborate *ab initio* calculations utilizing a microscopic solvent model would be required for further understanding the solvation effect since they employed a semiempirical level electronic structure theory with the dielectric continuum model.

The purpose of the present paper is to provide detailed analysis of the thermodynamic property for the keto-enol tautomerization of acetylacetone in solution based on the *ab initio* electronic structure calculations. We chose H₂O and

dimethyl sulfoxide (DMSO), and carbon tetrachloride (CCl_4), representing, respectively, protic polar, aprotic polar and nonpolar solvents. The solvation free energies in these solvents were analyzed by decomposing them into the enthalpic and entropic contributions based on the scheme proposed by Yu *et al.*^{24,25} The effect of changes in solute geometry and vibrations due to the solvation was also examined. The organization of the paper is as follows. In the following section, the theoretical methods employed are presented. In Sec. III, we present the results of calculations. The solvent effect on the solute geometries and vibrational frequencies are discussed. The thermodynamic analysis of the solvation free energies in the tautomerization is performed to study the stabilities of the keto and enol tautomers in solution. The origin of geometric change of the keto form is also discussed. Conclusions are summarized in Sec. IV.

II. THEORETICAL METHODS

A. RISM-SCF method

Since the details of the RISM-SCF method have been presented in the previous papers,^{6,7} we only describe the outline of theory pertinent to the calculations of the electron correlation energy of solute molecule and the thermodynamic analyses of solvation free energies.

In the RISM-SCF theory, the total free energy of the system considered is defined by

$$G = \langle \Psi | \hat{H}_{\text{gas}} + \Delta \hat{\mu}_{\text{sol}} | \Psi \rangle, \quad (1)$$

where Ψ is the solute electronic wave function and \hat{H}_{gas} is the electronic Hamiltonian of solute in the gas phase. The operator $\Delta \hat{\mu}_{\text{sol}}$ determines the excess chemical potential due to the solvation, which is the functional of the solute-solvent correlation functions $h_{\alpha\gamma}$, the direct correlation functions $c_{\alpha\gamma}$, and the t -bonds $t_{\alpha\gamma}$. Here, α and γ denote the interaction sites in solute and solvent molecules.

The variation of the free energy, Eq. (1), with respect to the solute molecular orbitals (MO) ϕ_i and the correlation functions $h_{\alpha\gamma}$, $c_{\alpha\gamma}$ and $t_{\alpha\gamma}$, automatically provides the Fock equation

$$\hat{F}_{\text{sol}} \phi_i = \varepsilon_i \phi_i, \quad (2)$$

the RISM Ornstein-Zernike (OZ) equation,

$$h_{uv} = w_u * c_{uv} * \omega_v + \rho \omega_u * c_{uv} * h_{vv}, \quad (3)$$

and the hypernetted chain (HNC) closure relation. In Eq. (3), the indices u and v denote the solute and solvent, ρ is the number density of solvent, and $\beta = 1/k_B T$ with k_B being the Boltzmann constant. w is the intramolecular correlation function that defines the molecular geometry. The solvent-solvent correlation function, h_{vv} , is determined by solving the RISM OZ equation for the pure solvent,

$$h_{vv} = \omega_v * c_{vv} * \omega_v + \rho \omega_v * c_{vv} * h_{vv}. \quad (4)$$

At convergence, the excess chemical potential^{26,27} is represented as

$$\Delta \mu_u = \frac{\rho}{2\beta} \sum_{\alpha \in u} \sum_{\gamma \in v} \int_0^\infty 4\pi r^2 dr (h_{\alpha\gamma}^2 - 2c_{\alpha\gamma} - h_{\alpha\gamma} c_{\alpha\gamma}). \quad (5)$$

The solvated Fock operator is given in the form

$$\hat{F}_{\text{sol}} = \hat{h} + 2\hat{J} - \hat{K} - \sum_{\alpha} V_{\alpha} \hat{b}_{\alpha}, \quad (6)$$

where \hat{h} , \hat{J} and \hat{K} are the usual one-electron, Coulomb and exchange operators, and \hat{b}_{α} is the population operator which generates the partial charge on the solute atomic site α . The averaged electrostatic potential acting on the site α is given by

$$V_{\alpha} = \rho \sum_{\gamma} q_{\gamma} 4\pi \int r g_{\alpha\gamma}(r) dr, \quad (7)$$

where $g_{\alpha\gamma}(r)$, $h_{\alpha\gamma}(r) + 1$ is the radial distribution function between the solute site α and the solvent site γ with the partial charge q_{γ} .

To calculate the electron correlation energy of the solute molecule in solution, we employ the Møller-Plesset (MP) perturbation expansion. We consider here up to the second-order correction. The Hamiltonian is partitioned into

$$H = \hat{H}_{\text{gas}} + \Delta \hat{\mu}_{\text{sol}} = \sum_i \hat{F}_{\text{sol}}(i) + \hat{V}, \quad (8)$$

where the zeroth order Hamiltonian is defined by the sum of solvated Fock operators and \hat{V} corresponds to the perturbation. Since $\Delta \hat{\mu}_{\text{sol}}$ and \hat{b}_{α} in the perturbation term \hat{V} are the one-electron operators, it is straightforward to show that the second-order correlation energy is represented by

$$E_{\text{MP2}}^{\text{sol}}(u) = \frac{1}{4} \sum_{abrs} \frac{|\langle ab || rs \rangle|^2}{\varepsilon_a + \varepsilon_b - \varepsilon_r - \varepsilon_s}, \quad (9)$$

where ε_a and ε_b are the occupied orbital energies, and ε_r and ε_s the unoccupied orbital energies, respectively. The integral $\langle ab || rs \rangle$ is the antisymmetrized two-electron integral.

All the *ab initio* calculations were performed at the restricted Hartree-Fock (RHF) level by using the $(9s5p1d/4s1p)/[3s2p1d/2s1p]$ basis set, which has a valence double zeta plus polarization quality.²⁸ The geometry of solute molecule was optimized using the analytical energy gradient technique²⁹ in each solvent studied. The MP2 calculations were repeated at the RISM-SCF optimized geometries to estimate the electron correlation effect.

All the parameters³⁰⁻³² employed for describing the solute-solvent interaction are summarized in Table I. Especially, for H_2O , the simple point charge (SPC)-like³³ model was used where the Lennard-Jones parameters, $\sigma = 1.0 \text{ \AA}$ and $\epsilon = 0.056 \text{ kcal/mol}$, were added on the H site. The Lennard-Jones parameters for the solute atoms³⁴ were also included in Table I. We used the standard combination rule to construct the solute-solvent van der Waals interaction. The temperature was set to be 295.15 K for CCl_4 , and 298.15 K for the other solvents.

We further calculated the harmonic vibrational frequencies of solute for estimating the zero-point energy of solute molecule, $E_{\text{ZPE}}(u)$, and the vibrational contribution to the free energy, ΔG_{vib} . The Hessian matrix was obtained by the

TABLE I. Parameters for solvents and solute.

Solvent ^a	Site	q	$\sigma/\text{\AA}$	$\epsilon/\text{kcalmol}^{-1}$
H ₂ O	H	0.41	1.000	0.056
	O	-0.82	3.166	0.155
DMSO	O	-0.459	2.80	0.0715
	S	0.139	3.40	0.238
	CH ₃	0.160	3.80	0.293
CCl ₄	C	-0.1616	3.2	0.10
	Cl	0.0404	3.4	0.26

Parameter for solute site ^b		$\sigma/\text{\AA}$	$\epsilon/\text{kcalmol}^{-1}$
C		3.562	0.1499
C(C ₂ and C ₅) ^c		3.296	0.1199
O		2.850	0.1999
H		2.450	0.0379

^aData from Refs. 30 and 31 for CCl₄, Ref. 32 for DMSO, and Ref. 33 for H₂O.

^bReference 34.

^cSee Fig. 1.

numerical differentiation of analytically calculated gradients of RISM-SCF free energy at the optimized geometry in each solvent.

B. Thermodynamic analysis

The solvation free energy is defined as the sum of the solute term ΔG_{solute} and the excess chemical potential $\Delta\mu_{\text{sol}}$. The solute term is given by

$$\Delta G_{\text{solute}} = \Delta E_{re} + \Delta \text{ZPE} + \Delta G_{\text{vib}}, \quad (10)$$

where ΔE_{re} is the solute electronic reorganization energy given as the change of solute electronic energy from the gas phase to the solution, and ΔZPE and ΔG_{vib} are the changes of the zero-point energy and vibrational free energy. It is noted that the change of solute electron correlation energy due to the solvation is included in ΔE_{re} .

The enthalpy and entropy contributions to the excess chemical potential were calculated using the method proposed by Yu *et al.*^{24,25} Taking the derivatives of h and c with respect to the solute or solvent density, ρ_u or ρ_v , the solvation energy $\Delta\epsilon_{u,\text{sol}}$ and the enthalpy $\Delta h_{u,\text{sol}}$ are calculated with the equations by the following:

$$\begin{aligned} \Delta\epsilon_{u,\text{sol}} = & \rho_v \sum_{\alpha=1}^{n_u} \sum_{\gamma=1}^{n_v} \int_0^\infty 4\pi r^2 dr U_{\alpha\gamma}(r) g_{\alpha\gamma}(r) \\ & + \frac{\rho_v^2}{2} \sum_{\gamma=1}^{n_v} \sum_{\gamma'=1}^{n_v} \int_0^\infty 4\pi r^2 dr U_{\gamma\gamma'}(r) \delta_{\rho_u} h_{\gamma\gamma'}(r), \end{aligned} \quad (11)$$

$$\begin{aligned} \Delta h_{u,\text{sol}} = & \Delta\epsilon_{u,\text{sol}} + T\alpha_{v,P} \left\{ \Delta\mu_{u,\text{sol}} + \frac{\rho_v^2}{2\beta} \sum_{\alpha=1}^{n_u} \sum_{\gamma=1}^{n_v} \int_0^\infty 4\pi r^2 dr \right. \\ & \left. \times [h_{\alpha\gamma}(r) \delta_{\rho_v} c_{\alpha\gamma}(r) - c_{\alpha\gamma}(r) \delta_{\rho_v} h_{\alpha\gamma}(r)] \right\}, \end{aligned} \quad (12)$$

where n_u and n_v denote the numbers of sites in the solute and solvent molecule, respectively. $U_{\alpha\gamma}$ and $U_{\gamma\gamma'}$ are the

solute-solvent and solvent-solvent site-site interaction potentials. $\alpha_{v,P}$ is the isobaric thermal expansion coefficient of the pure solvent. In the present study, the experimental data for $\alpha_{v,P}$,³⁵ $2.57 \times 10^{-4} \text{ K}^{-1}$ for H₂O, 9.28×10^{-4} for DMSO and 1.22×10^{-3} for CCl₄, respectively, were employed. The first term in the right hand side of Eq. (11) represents the solute-solvent interaction energy E_{uv} and the second is the cavity formation energy E_{cav} , which represents the solvent reorganization energy due to solvation.

The solvation entropy is defined by

$$\Delta S_{u,\text{sol}} = (\Delta h_{u,\text{sol}} - \Delta\mu_{\text{sol}})/T. \quad (13)$$

Based on the extended RISM theory,³⁶⁻³⁸ the first-order isothermal density derivatives to Eqs. (3) and (4) provide the relation

$$\begin{aligned} \delta_{\rho_\eta} \hat{h}_{ss'} = & \hat{w}_s \delta_{\rho_\eta} \hat{c}_{ss'} \hat{w}_{s'} + [\hat{w}_s \delta_{\rho_\eta} \hat{c}_{sv} + \hat{h}_{sv} \rho_v \delta_{\rho_\eta} \hat{c}_{vv}] \\ & \times \rho_v \hat{h}_{vs'} + \hat{h}_{s\eta} \hat{w}_\eta^{-1} \hat{h}_{\eta s'}, \end{aligned} \quad (14)$$

where \hat{h} , \hat{c} and \hat{w} represent h , c and w in k -space, respectively, with $\{s, s'\} = \{u, v\}$. The corresponding relation to the HNC closure is given by

$$\delta_{\rho_\eta} h_{\alpha\gamma}(r) = [\delta_{\rho_\eta} h_{\alpha\gamma}(r) - \delta_{\rho_\eta} c_{\alpha\gamma}^*(r)] [h_{\alpha\gamma}(r) + 1], \quad (15)$$

where η represents u or v , and $\delta_{\rho_\eta} \hat{c}^* = \delta_{\rho_\eta} \hat{c} - \hat{\phi}^\eta$, $\hat{\phi}^\eta = \delta_{\rho_\eta} \hat{\phi}$.

The free energy difference between the keto and enol tautomers is defined by

$$\begin{aligned} \Delta G(k-e) = & \Delta G_{\text{solute}}(k) - \Delta G_{\text{solute}}(e) + \Delta\mu_{\text{sol}}(k) \\ & - \Delta\mu_{\text{sol}}(e) + \Delta G_{\text{gas}}(k-e), \end{aligned} \quad (16)$$

where $\Delta G_{\text{gas}}(k-e)$ is the free energy difference in the gas phase. With the free energy partitioning scheme discussed above, the differences of the enthalpy and entropy terms between tautomers are easily derived.

The solvation enthalpy is defined by

$$\Delta H_{\text{sol}} = \Delta h_{u,\text{sol}} + \Delta E_{re} + \Delta E_{\text{vib}}^{\text{sol}} - \Delta E_{\text{vib}}^{\text{gas}} - 3k_B T, \quad (17)$$

and then, the enthalpy difference is calculated by

$$\Delta H(k-e) = \Delta H_{\text{sol}}(k) - \Delta H_{\text{sol}}(e) + \Delta H_{\text{gas}}(k-e), \quad (18)$$

where $\Delta H_{\text{gas}}(k-e)$ is the energy difference in the gas phase including the vibrational energy. The enthalpy difference, $\Delta H(k-e)$, is related to $\Delta G(k-e)$ by

$$\Delta G(k-e) = \Delta H(k-e) - T\Delta S(k-e), \quad (19)$$

where $\Delta S(k-e)$ is the entropy difference.

III. RESULTS AND DISCUSSION

A. Solute property

Figure 1 shows the geometries of the keto and enol tautomers of acetylacetone along with the site numberings. The optimized geometric parameters in the gas phase and in each solvent are summarized in Table II.

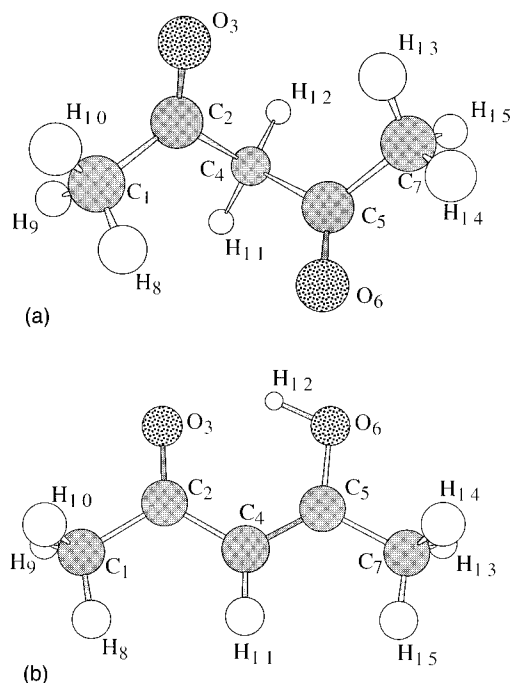


FIG. 1. Molecular geometry and site assignment for tautomers of acetylacetone (a) keto form (b) enol form.

For the keto tautomer, we found the two geometries in the gas phase; one with the dihedral angles, τ_{3256} , of 140.4 and the other of 102.4°, respectively. The former is more stable than the latter by 1.87 kcal/mol at the MP2 level, which is consistent with the result by Dannenberg *et al.*,¹⁹ 1.1 kcal/mol. We also obtained two optimized structures in CCl₄, and their geometries are very close to those in the gas phase as seen in Table II. Since the conformer with $\tau_{3256} = 140.4^\circ$ is lower in energy by 1.35 kcal/mol than the other with $\tau_{3256} = 101.6^\circ$, we consider only the former in later discussion.

TABLE II. Selected geometric parameters for both tautomers in the gas phase and solutions. (Units: R in Å, τ and θ in degree.)

Keto form	Gas phase	In CCl ₄	In DMSO	In H ₂ O
$R_{24 \text{ or } 45}^a$	1.529 (1.529) ^b	1.527 (1.526) ^b	1.520	1.522
$R_{12 \text{ or } 57}^a$	1.510 (1.508)	1.508 (1.506)	1.504	1.504
$R_{23 \text{ or } 56}^a$	1.195 (1.194)	1.195 (1.194)	1.197	1.213
τ_{3256}	140.4 (102.4)	140.4 (101.6)	75.2	56.4
θ_{245}	108.6 (109.9)	108.6 (110.0)	112.8	115.8
R_{36}	3.787 (3.259)	3.783 (3.249)	2.940	2.763
Enol form				
R_{12}	1.514	1.510	1.509	1.508
R_{23}	1.218	1.217	1.223	1.246
R_{24}	1.459	1.456	1.454	1.455
R_{45}	1.356	1.355	1.355	1.368
R_{56}	1.316	1.315	1.318	1.329
R_{57}	1.497	1.496	1.495	1.496
θ_{245}	121.5	121.4	121.7	122.8
τ_{12-654}	0.0	0.0	0.0	0.0
R_{6-12}	0.961	0.960	0.961	0.973
$R_{3 \cdots 12}$	1.685	1.680	1.672	1.727

^aAveraged values.

^bParentheses represent parameters for the other keto conformer.

TABLE III. Dipole moment in the gas phase and solutions (units in D).

	keto	enol
CCl ₄	1.752 (3.767) ^a	3.186
DMSO	6.014	3.928
H ₂ O	8.863	5.311
gas	1.744 (3.724) ^a	3.157

^aValues in parentheses are for the other keto conformer ($\tau_{3256} = 102.4^\circ$).

The geometry of the keto tautomer undergoes a drastic change in polar solvents. The stable conformer with a larger dihedral angle observed in the gas phase and CCl₄ disappeared and the torsional angle, τ_{3256} , significantly decreased to 56.4 in H₂O and to 75.2° in DMSO. The calculated torsional angle in H₂O is similar to the predicted value, 59°, by Cramer and Truhlar²³ with the semiempirical calculations. These results indicate that the dihedral angle changes so as to increase the solute dipole moment with the increase of solvent polarity. Table II shows that the C=O bond length in the carbonyl group becomes longer in polar solvent, though the average C—C bond length becomes slightly short compared with that in the gas phase. The bending angle, θ_{245} , also increases, which is because the repulsion between lone pair electrons in the two carbonyl groups becomes large as the dihedral angle decreases, and thus the bending angle becomes wide in order to reduce such repulsive interaction. The origin of these geometric changes in polar solvents will be discussed in Sec. III D.

In the enol tautomer, the geometric change due to the solvation is smaller than that in the keto one. All the atoms except for the methyl hydrogens lie in the same plane in all the solvents as in the gas phase. The change of bending angle, θ_{245} , is also small. As seen in Table II, R_{23} and R_{56} become longer in the polar solvents than in the gas phase, while the change of their lengths is small in CCl₄. It is considered that these changes occur in order to make the solute dipole moment increase in DMSO and H₂O. The distance $R_{3 \cdots 12}$ characterizing the intramolecular hydrogen bonding was calculated to be 1.685 Å in the gas phase, which is comparable to the experimental value, 1.626 Å.¹⁰ While $R_{3 \cdots 12}$ becomes slightly shorter in CCl₄ and DMSO compared with the gas phase value, it is elongated by 0.04 Å in H₂O, indicating that the intramolecular hydrogen bonding is weakened in aqueous solution. The intramolecular hydrogen bonding in the enol remains intact even in polar solvents, these results being consistent with the experimental observation by Emsley and Freeman.¹⁵

The calculated dipole moments in the solvents as well as in the gas phase are shown in Table III. The dipole moment of the keto is larger than that of the enol in the gas phase. This tendency agrees with the previous studies.^{13,23} In solutions, the dipole moment of the keto form is enhanced as the solvent polarity increases since the dihedral angle between the planes containing two carbonyl groups becomes smaller. For the enol, the degree of enhancement of dipole moment induced by the solvation is not so large, since such a marked change in geometry observed in the keto form does not oc-

TABLE IV. Selected solute vibrational frequencies.^a

Keto form	Gas phase	In CCl ₄	In DMSO	In H ₂ O
C ₂ C ₄ C ₅ bending	152.3	153.8	128.3	106.0
C=O antisymmetric	1986.0	1988.5	1964.0	1862.8
C=O symmetric	2009.2	2011.8	2001.9	1923.6
Enol form				
C ₄ -C ₅ stretching	1779.2	1771.7	1751.9	1669.8
C ₂ -O ₃ stretching	1904.4	1894.4	1862.7	1765.3
O ₆ -H ₁₂ stretching	3871.4	3871.2	3846.5	3686.8

^aUnits in cm⁻¹.

cur. The dipole moment, however, is appreciably larger in H₂O than in the gas phase.

The harmonic vibrational frequencies were calculated in all the solvents considered, as well as in the gas phase. The frequencies in CCl₄ were close to the gas phase values, while those in H₂O changed appreciably from the gas phase ones. In Table IV, we only showed the vibrations which undergo large frequency shifts, more than 20 cm⁻¹, due to solvation. In the keto, the frequency of C₂C₄C₅ bending vibration decreases with increasing the solvent polarity, which is consistent with the result that bond angle θ_{245} becomes large by the solvation. The frequencies for C=O stretching are remarkably reduced by ~ 100 cm⁻¹ in H₂O. This is because the hydrogen bonding between the carbonyl O and water H atoms is formed in aqueous solution and thus the C=O bond distances lengthen. Experimentally, it was observed that the C=O stretching frequency was lower by about 100 cm⁻¹ in aqueous solution.³⁹⁻⁴¹ In the enol, the frequencies of C₄C₅ and C₂O₃ stretching modes decrease in the polar solvents. In particular, the shifts of these frequencies are more than 100 cm⁻¹ in the aqueous solution, corresponding to the significant increases of R_{45} and R_{23} distances as seen in Table II. The OH stretching frequency also decreases in the polar solvents. Although the frequency change is only 30 cm⁻¹ in DMSO, it is reduced by 190 cm⁻¹ in H₂O, indicating that a strong hydrogen bond is formed between the water O atom and the H atom of the OH group in the enol tautomer.

B. Keto-Enol equilibrium

Table V shows the calculated free energy differences between the keto and enol tautomers along with the available experimental values. In H₂O, the free energy of the keto form was calculated to be lower than that of the enol by -1.37 kcal/mol, which is in good agreement with the experiment, -1.18 kcal/mol. For DMSO solution, the stability of the two tautomers became comparable to each other, 0.14 kcal/mol, as in the experiment. The free energies were also very close in CCl₄, which is slightly different from the experiment where the enol form is more stable than the keto by 1.76 kcal/mol. This discrepancy in the free energy difference in CCl₄ solution may come from the underestimation of solute electronic energy difference between the tautomers. In the present calculation, the electronic energy of the enol form is lower than that of the keto only by 1.04 kcal/mol in the gas phase, which provides the free energy difference of -0.69 kcal/mol. As shown by Bauer and Wilcox,⁴² the elec-

TABLE V. Differences of total free energies between the Keto and enol and their components.

Solvent	$\Delta G(k-e)$	$\Delta H(k-e)^a$	$T\Delta S(k-e)^a$	$\Delta G_{\text{exp}}(k-e)^b$
H ₂ O	-1.37	-6.05 (2.7 \pm 0.3)	-4.68 (3.7)	-1.18 (-0.98)
DMSO	0.14	0.55 (1.8 \pm 0.2)	0.41 (1.5)	-0.16 (0.29)
CCl ₄	0.11	1.02 (2.5 \pm 0.3)	0.91 (0.80)	1.76 (1.74)
Gas	-0.69	2.20 ^c
Components of $\Delta G(k-e)$				
Solvent	$\Delta E_{\text{sol}}(k-e)^d$	$\Delta \text{ZPE}(k-e)$	$\Delta G_{\text{vib}}(k-e)$	$\mu_{\text{sol}}(k-e)$
H ₂ O	17.71 (11.57)	-0.47	-1.08	-17.53
DMSO	6.46 (3.08)	-0.89	-1.27	-4.16
CCl ₄	1.00 (-0.35)	-0.87	-0.98	0.96
Gas	1.04 (-0.35)	-0.84	-0.89	...

^aValues in parentheses are the experimental data in Ref. 14.^bData from Ref. 15. Data in parentheses from Ref. 14.^cReference 13.^dValues in parentheses are the RHF level results.

tronic energy difference becomes larger by employing the complete basis set method. Considering that the solute geometries are very similar to those in the gas phase, and the electric field is weak in CCl₄, the error in the gas phase energy is the origin of small difference in the free energies for CCl₄ solution.

We further tabulated the components of free energy differences in Table V. The electronic energy difference, $\Delta E_{\text{sol}}(k-e)$, increases with the solvent polarity, which is mainly attributed to the geometric change of the keto form due to the solvation. It was also found that the electron correlation energy becomes smaller in polar solvents than in the gas phase and such a solvent effect is remarkable in the keto form. This is because the electrostatic potential coming from the surrounding solvent enlarges the energy gap between occupied and unoccupied MOs of the solute, and thus the correlation energy is reduced for the keto due to strong solvation. As shown in Table IV, there are some solute normal vibrations whose frequencies are reduced in polar solvents, and thus the zero-point energy becomes smaller in solution than that in the gas phase. The calculated zero-point energy changes due to the solvation were 0.07, -0.39 and -0.75 kcal/mol in CCl₄, DMSO and H₂O, respectively, for the keto, while those for the enol were -0.04, -0.34 and -1.12 kcal/mol. The relatively larger negative value of the enol ZPE attributed to the formation of the hydrogen bonding with H₂O molecules is remarkable, which provides the smaller difference in ZPEs between the tautomers in water compared to the other solvent as well as the gas phase (Table V). The solvent effect on the vibrational frequencies also changes the solute vibrational contribution to the free energy difference, $\Delta G_{\text{vib}}(k-e)$. As shown in Table V, $\Delta G_{\text{vib}}(k-e)$ is negative in all the solvents as well as in the gas phase, indicating that the keto form has low frequency vibrational modes more than the enol. It is worth noting that the present calculations reproduced the experimental estimates of the free energy differences in the solutions fairly well by including the solute electronic reorganization energies and vibrational free energies.

TABLE VI. Solvation enthalpy terms. (Units in kcal/mol.)

Solvent	Keto					Enol				
	ΔH_{sol}^a	$\Delta h_{u,\text{sol}}$	E_{uv}	E_{cav}	Experimental	ΔH_{sol}^a	$\Delta h_{u,\text{sol}}$	E_{uv}	E_{cav}	Experimental
H ₂ O	5.02	-17.23	-84.72	35.67	-10.6	11.56	6.48	-46.60	19.81	-11.1
DMSO	-13.95	-17.88	-40.10	7.49	-9.8	-14.01	-12.54	-30.63	3.97	-9.4
CCl ₄	-5.38	-2.61	-18.56	1.47	-8.2	-5.91	-3.82	-19.40	1.63	-8.5

^aValues include MP2 energies.

The keto-enol difference of the excess chemical potentials, $\mu_{\text{sol}}(k-e)$, becomes more negative with the solvent polarity. This implies that the keto is more stabilized by the solvation, which is consistent with large enhancement of the keto dipole moment in polar solvent accompanied by the drastic geometric change. As seen in Table V, the stabilization by $\mu_{\text{sol}}(k-e)$ is comparable to the destabilization of solute electronic energy, $\Delta E_{\text{sol}}(k-e)$, in the aqueous solution.

C. Thermodynamic analysis

The solvation enthalpies, ΔH_{sol} , of the two tautomers in solutions are shown in Table VI. In DMSO and CCl₄, the calculated values are comparable to the experimental ones. However, we found large discrepancies between the calculation and experiment for those in H₂O. Although the calculated enthalpies are positive for both the tautomers, the experiments provided negative values of the enthalpies, which are close to those for DMSO and CCl₄ solutions. Moreover, the enol is more enthalpically unstable than the keto by 6.5 kcal/mol in the calculations, while the experimental estimate is reversed.

In order to clarify the origins of such discrepancies in the enthalpies for the aqueous solution, we examined the components of ΔH_{sol} , which are included in Table VI. According to Eq. (17), the solvation enthalpy is composed of two contributions; one is $\Delta h_{u,\text{sol}}$ coming from the solute-solvent interaction and another is the solute term including the electronic and vibrational contributions, as well as those from the translation and rotation in the gas phase. As seen in Table VI, the differences in the solute-solvent term $\Delta h_{u,\text{sol}}$ are rather small and are further cancelled out by the solute terms to give similar values of ΔH_{sol} for the two tautomers in DMSO and CCl₄. On the other hand, in the aqueous solution, there is a large difference in $\Delta h_{u,\text{sol}}$ between the tautomers, and the solvation enthalpies ΔH_{sol} of the enol are still larger than those of the keto even after including the solute terms. Considering that the errors in the solute terms are relatively small because we estimated them by *ab initio* calculations, the discrepancies should be attributed to the solute-solvent term $\Delta h_{u,\text{sol}}$.

As in Eq. (12), $\Delta h_{u,\text{sol}}$ is given as the sum of two terms. The first term ϵ_{sol} , the solvation energy, is further decomposed into the solute-solvent interaction energy E_{uv} and the cavity formation energy (solvent reorganization energy) E_{cav} , i.e., Eq. (11). Yu *et al.*⁴³ pointed out that the RISM integral equation theory provides comparable results for E_{uv} to the computer simulations, while E_{cav} is overestimated with

the HNC approximation in aqueous solution. The present calculations yielded considerably large values of E_{uv} in water in comparison with those in DMSO and CCl₄, indicating the existence of hydrogen bonding in solvent-solvent and solute-solvent in the aqueous solution causes an overestimation of E_{cav} , while such an effect is small in DMSO and CCl₄, typical aprotic solvents, having a small ability of hydrogen bonding. It is noted that the second term in Eq. (12) might be overestimated in the present treatments, because this term also originated from the reorganization of solvent water.

Only the overestimations of E_{cav} and the second term in Eq. (12) may not resolve a large discrepancy in the calculated solvation enthalpies between the tautomers because the error in E_{cav} is considered to be larger for the keto than the enol. As pointed out by Spencer *et al.*,¹⁴ the enol tautomer can be enthalpically stabilized through self-association. Although the self-association of enol might be one of the possibilities for interpreting the discrepancy between the present calculation and the experiment for both the tautomers in the solvation enthalpies, we have not examined this possibility because such an effect is beyond the scope of the present study.

The changes of the enthalpy and entropy terms caused by the keto-enol tautomerization are shown in Table V. The calculated results are comparable to the experiments for DMSO and CCl₄ solutions as in the case of solvation enthalpies discussed above. For the aqueous solution, the calculations gave the enthalpy and entropy changes with the opposite signs to the experiments. The calculated results imply that the keto form is enthalpically more stable but entropically more unstable than the enol, which can be easily understood considering the stronger solute-solvent interaction in the keto.

D. Driving force for the geometric change of the keto tautomer in solutions

As shown in Sec. III A, the keto tautomer undergoes a large geometry change going from the gas phase to the polar solvents. We discuss here the driving force to cause such a change in geometry. For this purpose, the free energy ΔG and solvation enthalpy ΔH_{sol} calculated at the gas phase optimized geometry, hereafter denoted as **a**, were compared with those in the polar solvents, **b**, and the results are summarized in Table VII. For the geometry in the gas phase, we took the optimized one with a smaller torsional angle ($\tau_{3256}=102.4^\circ$). Note that the solute vibrational contributions were omitted in calculating ΔG and ΔH_{sol} , though the electron correlation energies were included.

TABLE VII. $\Delta G(\mathbf{b}-\mathbf{a})$, $\Delta H(\mathbf{b}-\mathbf{a})$ and $T\Delta S(\mathbf{b}-\mathbf{a})$ with \mathbf{a} the optimized geometry in gas phase and \mathbf{b} the optimized geometry in solution. (Units in kcal/mol.)^a

Solvent	$\Delta G(\mathbf{b}-\mathbf{a})$	$\Delta H(\mathbf{b}-\mathbf{a})^b$	$T\Delta S(\mathbf{b}-\mathbf{a})$
DMSO	-0.44	0.58	1.02
H ₂ O	-3.35	-4.81	-1.46

^aFor all values, the electron correlation energies are included.

^b $\Delta H_{\text{gas}}(\mathbf{b}-\mathbf{a})$ s are 0.67 in DMSO, 0.75 kcal/mol in H₂O.

The free energy ΔG at \mathbf{b} is more stable than that of \mathbf{a} because the geometry \mathbf{b} corresponds to the minimum free energy point in each solvent. However, the difference of the enthalpies between \mathbf{a} and \mathbf{b} obtained with Eq. (18), $\Delta H(\mathbf{b}-\mathbf{a})$, is positive in DMSO, indicating that the geometry \mathbf{b} is enthalpically unstable compared with \mathbf{a} , and thus the geometric change observed for DMSO solution is driven by the entropy term. In the aqueous solution, the situation is quite different from the DMSO case: the calculated $\Delta H(\mathbf{b}-\mathbf{a})$ is -4.81 kcal/mol and the entropy change is also negative, as going from \mathbf{a} to \mathbf{b} . We can thus conclude that the enthalpy term is responsible for causing the geometric change in H₂O.

In order to clarify such a difference of the driving forces for the geometric change between the DMSO and aqueous solutions, we examined the solvation structures, i.e., the radial distribution functions (rdfs). Figure 2 compares the rdfs between the O₃ site of acetylacetone and the water H site obtained at the geometries \mathbf{a} and \mathbf{b} because the solute O₃ and O₆ sites participate in the solute-solvent interaction most strongly. In DMSO, the height of the first peak is almost the same between \mathbf{a} and \mathbf{b} , as seen in Fig. 2(a). This means that the solvation structure around the solute does not undergo a large modification by the geometric change from \mathbf{a} to \mathbf{b} and the positive enthalpy change, $\Delta H(\mathbf{b}-\mathbf{a})$, is attributed to the increase of solute electronic energy. On the contrary, the solvation becomes stronger after the geometric change in the aqueous solution. The first peak is higher at \mathbf{b} than \mathbf{a} , as illustrated in Fig. 2(b), which implies that the hydrogen bonding becomes strong by the geometry change, and the stabilization due to the increase of solute-solvent interaction energy overcomes the increase of solute electronic reorganization energy. The difference of solvation structures between the DMSO and aqueous solutions can be rationalized if we see the change of the partial charges on the O₃ and O₆ sites caused by the solute geometric change from \mathbf{a} to \mathbf{b} : the partial charges change from -0.74 to -0.79 in H₂O, while the change in DMSO is very small, from -0.62 to -0.63.

IV. CONCLUSIONS

In the present paper, we studied the keto-enol tautomerization equilibrium of acetylacetone in CCl₄, DMSO and H₂O with the RISM-SCF method. The solvation free energies were analyzed by decomposing them into the enthalpy and entropy contributions as well as the solute electronic and vibrational ones. The conclusions derived from the calculations are summarized as follows:

- (1) The geometry of keto tautomer undergoes a large change in polar solvents from that in the gas phase. Especially,

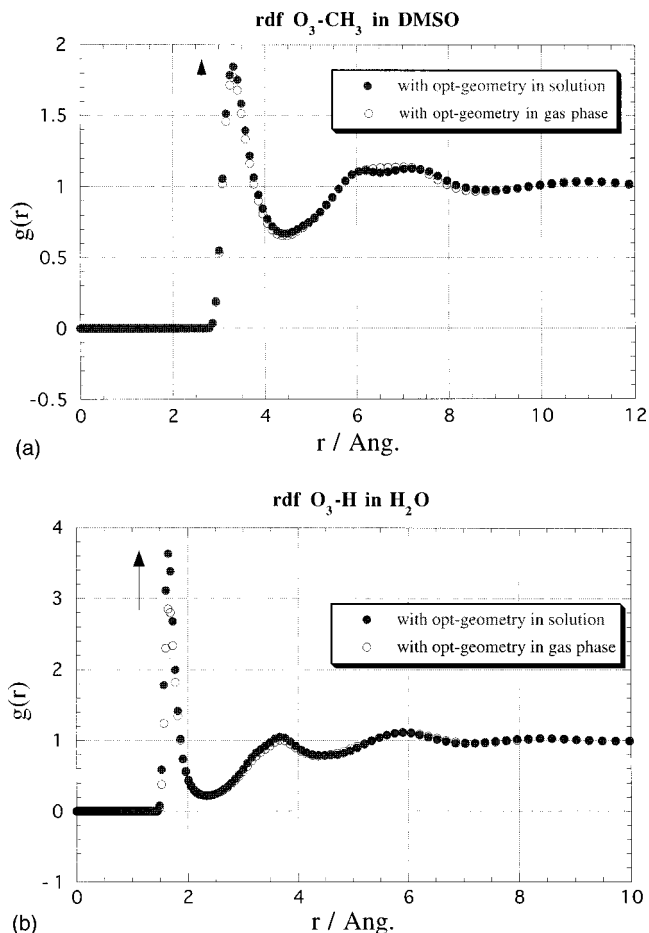


FIG. 2. Radial distribution functions between the O₃ site of the keto and the solvent sites. Arrows indicate the change of the first peak. (a) O-CH₃ (solvent: DMSO), (b) O-H (solvent: H₂O).

the dihedral angle between the planes containing two carbonyl groups becomes small, 56.4 and 75.2° in H₂O and DMSO, respectively. In CCl₄, the geometry was almost the same as in the gas phase. For the enol, the solvent induced geometry change was rather small even in polar solvents.

- (2) The calculated keto-enol free energy difference in solution was in good agreement with the experiments, including the vibrational free energy difference and zero-point energy contributions as well as the electron correlation effect of solute. It was found that the equilibrium shifts to the keto form in aqueous solution while the enol is still dominant in CCl₄ as in the gas phase.
- (3) The calculated solvation enthalpies for both tautomers were comparable to the experimental estimates in CCl₄ and DMSO. However, we observed a large discrepancy in the solvation enthalpies in H₂O between the calculations and experiments, which was attributed to the overestimation of the cavity formation energy in water solvent.
- (4) The origin of a large geometric change of the keto form in polar solvents was examined. It was found that such a geometric change is driven by the enthalpy term for aqueous solution while the entropy term is important in DMSO.

ACKNOWLEDGMENTS

We thank Dr. A. Morita for valuable discussions. This work was supported by the Grant in Aid for Scientific Research from the Ministry of Education.

- ¹W. L. Jorgensen, *Acc. Chem. Res.* **22**, 184 (1989).
- ²J. Gao, *Acc. Chem. Res.* **29**, 298 (1996).
- ³J. Tomasi and M. Persico, *Chem. Rev.* **94**, 2027 (1994).
- ⁴T. Ishida, F. Hirata, H. Sato, and S. Kato, *J. Phys. Chem. B* **102**, 2045 (1998).
- ⁵M. W. Wong, K. B. Wiberg, and M. J. Frisch, *J. Am. Chem. Soc.* **114**, 1645 (1992).
- ⁶S. Ten-no, F. Hirata, and S. Kato, *Chem. Phys. Lett.* **214**, 391 (1993).
- ⁷S. Ten-no, F. Hirata, and S. Kato, *J. Chem. Phys.* **100**, 7443 (1994).
- ⁸J. Emsley, *Struct. Bonding (Berlin)* **57**, 147 (1984).
- ⁹A. H. Lowrey, C. George, P. D'Antonio, and J. Karle, *J. Am. Chem. Soc.* **93**, 6399 (1971).
- ¹⁰K. Iijima, A. Ohnogi, and S. Shibata, *J. Mol. Struct.* **156**, 111 (1987).
- ¹¹J. Powling and H. J. Bernstein, *J. Am. Chem. Soc.* **73**, 4353 (1951).
- ¹²S. L. Wallen, C. R. Yonker, C. L. Phelps, and C. M. Wai, *J. Chem. Soc., Faraday Trans.* **93**, 2391 (1997).
- ¹³M. M. Folkendt, B. E. Weiss-Lopez, J. P. Chauvel, Jr., and N. S. True, *J. Phys. Chem.* **89**, 3347 (1985).
- ¹⁴J. N. Spencer, E. S. Holmboe, M. R. Kirshenbaum, D. W. Firth, and P. B. Pinto, *Can. J. Chem.* **60**, 1178 (1982).
- ¹⁵J. Emsley and N. J. Freeman, *J. Mol. Struct.* **161**, 193 (1987).
- ¹⁶W. Blokzijl and J. B. F. N. Engberts, *J. Chem. Soc., Perkin Trans. 2*, 455 (1994).
- ¹⁷E. Iglesias, *J. Chem. Soc., Perkin Trans. 2*, 431 (1997).
- ¹⁸M. T. Rogers and J. L. Burdett, *Can. J. Chem.* **43**, 1516 (1965).
- ¹⁹J. J. Dannenberg and R. Rios, *J. Phys. Chem.* **98**, 6714 (1994).
- ²⁰G. Buemi and C. Gandolfo, *J. Chem. Soc., Faraday Trans. 2* **85**, 215 (1989).
- ²¹M. Karelson, *Adv. Quantum Chem.* **28**, 141 (1997).
- ²²M. A. Rios and J. Rodríguez, *J. Mol. Struct.: THEOCHEM* **204**, 137 (1990).
- ²³C. J. Cramer and D. G. Truhlar, in *Solvent Effects and Chemical Reactivity*, edited by O. Tapia and J. Bertrán (Kluwer, Dordrecht, 1996).
- ²⁴H. A. Yu and M. Karplus, *J. Chem. Phys.* **89**, 2366 (1988).
- ²⁵H. A. Yu, B. Roux, and M. Karplus, *J. Chem. Phys.* **92**, 5020 (1990).
- ²⁶S. J. Singer and D. Chandler, *Mol. Phys.* **55**, 621 (1985).
- ²⁷D. A. Zichi and P. J. Rossky, *J. Chem. Phys.* **84**, 1712 (1986).
- ²⁸T. H. Dunning, Jr., and P. J. Hay, in *Modern Electronic Structure Theory*, edited by H. F. Schaefer, III (Plenum, New York, 1977).
- ²⁹H. Sato, F. Hirata, and S. Kato, *J. Chem. Phys.* **105**, 1546 (1996).
- ³⁰L. J. Lowden and D. Chandler, *J. Chem. Phys.* **61**, 5228 (1974).
- ³¹T.-M. Chang, K. A. Peterson, and L. X. Dang, *J. Chem. Phys.* **103**, 7502 (1995).
- ³²A. Luzar, A. K. Soper, and D. Chandler, *J. Chem. Phys.* **99**, 6836 (1993).
- ³³H. J. C. Brendsen, J. P. M. Postma, W. F. von Gustern, and J. Hermas, in *Intermolecular Forces*, edited by B. Pullman (Reidel, Dordrecht, 1981).
- ³⁴S. J. Weiner, P. A. Kollman, D. A. Case, U. C. Singh, C. Ghio, G. Alagona, S. Profeta, Jr., and P. Weiner, *J. Am. Chem. Soc.* **106**, 765 (1984).
- ³⁵J. A. Riddick, W. B. Bunger and T. K. Sakano, *Organic Solvents*, 4th ed. (Wiley-Interscience, New York, 1986).
- ³⁶F. Hirata and P. J. Rossky, *Chem. Phys. Lett.* **83**, 329 (1981).
- ³⁷F. Hirata, B. M. Pettitt, and P. J. Rossky, *J. Chem. Phys.* **77**, 509 (1982).
- ³⁸F. Hirata, P. J. Rossky, and B. M. Pettitt, *J. Chem. Phys.* **78**, 4133 (1983).
- ³⁹R. Mecke and E. Funck, *Z. Elektrochem.* **60**, 1124 (1956).
- ⁴⁰K. L. Wierzchowski and D. Shugar, *Spectrochim. Acta* **21**, 943 (1965).
- ⁴¹E. E. Ernstbrunner, *J. Chem. Soc. A*, 1558 (1970).
- ⁴²S. H. Bauer and C. F. Wilcox, *Chem. Phys. Lett.* **279**, 122 (1997).
- ⁴³H. A. Yu, B. M. Pettitt, and M. Karplus, *J. Am. Chem. Soc.* **113**, 2425 (1991).